Magnetic nanocarriers for the specific delivery of siRNA: Contribution of breast cancer cells active targeting for down-regulation efficiency

Jonathan Bruniaux, Emilie Allard-Vannier, Nicolas Aubrey, Z. Lakhrif, Sanaa Ben Djemaa, Sahar Eljack, Hervé Marchais, Katel Hervé-Aubert, Igor Chourpa, Stephanie David

Magnetic nanocarriers for the specific delivery of siRNA: contribution of breast cancer cells active targeting for down-regulation efficiency

J. Bruniaux[1], E. Allard-Vannier[1], N. Aubrey[2], Z. Lakhrif[2], S. Ben Djemaa[1], S. Eljack[1], H. Marchais[1], K. Hervé-Aubert[1], I. Chourpa[1] and S. David[1]*

[1] Université de Tours, EA6295 « Nanomédicaments et Nanosondes », Tours, 37200, France

[2] Université de Tours, UMR1282, INRA, « Infectiologie et Santé Publique », équipe BIOMAP, Tours, 37200, France

*corresponding author : Université de Tours, EA 6295 Nanomédicaments et Nanosondes, Laboratoire de pharmacie galénique, Faculté de pharmacie, 31 avenue Monge, 37200 Tours, France. Tel.: +33 247 367199; fax: +33 247 367198. E-mail address: stephanie.david@univ-tours.fr

Keywords: small interfering RNA (siRNA), superparamagnetic iron oxide nanoparticles (SPION), scFv anti-HER2, survivin,

Abreviations:

Charge ratio of positive polymer's amino groups to negative siRNA's phosphate groups, CR; Dulbecco's Modified Eagle Medium, DMEM; Enhanced Permeability and Retention, EPR; human epidermal growth factor receptor-2, HER2; monoclonal antibody, mAb; nanoparticle, NP; single-chain antibody fragments, scFv; Stealth Fluorescent Particles, SFP; small interfering RNA, siRNA; Stealth Magnetic siRNA Nanovectors, S-MSN; superparamagnetic iron oxide nanoparticles, SPION; Targeted

Stealth Fluorescent Particles, T-SFP; Targeted Stealth Magnetic siRNA Nanovectors, TS-MSN;

Abstract

The association between superparamagnetic iron oxide nanoparticles (SPION), carrying small interfering RNA (siRNA) as therapeutic agents and humanized anti-human epidermal growth factor receptor-2 (HER2) single-chain antibody fragments (scFv) for the active delivery into HER2-overexpressing cells appears as an interesting approach for patients with HER2-overexpressing advanced breast cancer. The obtained Targeted Stealth Magnetic siRNA Nanovectors (TS-MSN) are formulated by combining: (i) the synthesis protocol of Targeted Stealth Fluorescent Particles (T-SFP) which form the core of TS-MSN and (ii) the formulation protocol allowing the loading of T-SFP with polyplexes (siRNA and cationic polymers). TS-MSN have suitable physico-chemical characteristics for intravenous administration and protect siRNA against enzymatic degradation up to 24h. The presence of HER2-targeting scFv on TS-MSN allowed an improved internalization (3 – 4 times more compared to untargeted S-MSN) in HER2-overexpressing breast cancer cells (BT-474). Furthermore, anti-survivin siRNA delivered by TS-MSN in HER2-negative breast-cancer control cells (MDA-MB-231) allowed significant down-regulation of the targeted anti-apoptotic protein of about 70%. This protein down-regulation increased in HER2+ cells to about 90% (compared to 70% with S-MSN in both cell lines) indicating the contribution of the HER2-active targeting. In conclusion, TS-MSN are promising nanocarriers for the specific and efficient delivery of siRNA to HER2-overexpressing breast cancer cells.

1. Introduction

Breast cancer is the most common cancer and the leading cause of cancer mortality in women worldwide. In 2012, 25% of all cancers recorded worldwide are represented by new breast cancer cases (Ferlay et al., 2015). Approximately 20% of breast cancer are caused by overexpression of the human epidermal growth factor receptor 2 (HER2) (Anhorn et al., 2008; Slamon et al., 1989; Steinhauser et al., 2006). This HER2 overexpression is currently associated with more aggressive tumor behavior and poorer clinical outcomes (Slamon et al., 1989). Treatment strategies for patients with HER2 positive advanced breast cancer have progressed significantly over the past few decades. The outcome of these patients has been improved with the introduction of multiple successful anti-HER2 therapies, including anti-HER2 monoclonal antibody (mAb, trastuzumab) (Swain et al., 2015; Verma et al., 2012), antibody-drug conjugate (ado trastuzumab emtansine or T-DM1) and tyrosine kinase inhibitor (lapatinib). The market introduction of four trastuzumab biosimilars in 2018 underlines the great interest of this humanized monoclonal antibody for the targeting of HER2 receptors (Santos et al., 2019). However, many HER2-overexpressing breast cancer patients do not respond to anti-HER2 mAb treatment alone (Marty et al., 2005) and development of resistance and disease recurrence continue to be the major clinical challenges as it occurs in more than 50% of treated patients. These clinical problems underline the need of alternative therapeutic strategies combined to anti-HER2 therapies.

RNA interference strategy using small interfering RNA (siRNA) is an attractive and innovative strategy to inhibit targeted proteins involved in treatment resistance. The first RNA interference drug based on siRNA, Patisiran, was approved by the US Food and Drug Administration in 2018 and other siRNA drugs are already used in

clinical trials (Kaczmarek et al., 2017; Ledford, 2018). However, their development as therapeutics is limited by several hurdles including (i) weak biostability as a consequence to nucleases digestion, (ii) poor uptake in cancer cells and, (iii) non-specific biodistribution. Therefore, the effective, targeted and safe delivery of siRNAs across the cell membrane to the cytoplasm remains a main obstacle that could be overcome by the complexation of siRNA with a nanosized cargo called nanoparticle (NP) (Wang et al., 2017, Ben Djemaa et al., this issue).

Passive targeting is known as accumulation of NP at the tumor site at high concentrations due to the pathophysiological differences between normal tissues and tumor tissues (Enhanced Permeability and Retention (EPR) effect) (Jee et al., 2012). In addition, active targeting is investigated through molecular recognition by conjugation of targeting moieties onto NP to obtain targeted delivery to specific cells, tissues or organs (Chattopadhyay et al., 2012; Slavoff and Saghatelian, 2012). Cancer cells express different molecular targets (antigens and/or receptors) than do normal cells and tissues. While some of these molecules are down-regulated, others are either newly expressed or significantly up-regulated on the surface of target cells, thus offering possibility of targeting strategies (Allen, 2002). Therefore, biological ligands such as antibodies are associated to nanovectors (Tatiparti et al., 2017). For the NP targeting function, a single-chain variable fragment (scFv) of trastuzumab offers several advantages over the whole antibody, mainly lower immunogenicity due to its reduced size (~27 kDa compared to 150kDa for the whole mAb) (Alric *et al*, 2018).

The purpose of this study was to develop Targeted Stealth Magnetic siRNA Nanovectors (TS-MSN) as a novel approach in breast cancer diagnosis and treatment to achieve maximal therapeutic benefit of anti-cancer siRNA. To combine

targeted cancer imaging and therapy, we used superparamagnetic iron oxide nanoparticles (SPION) that can provide imaging ability through MRI. SPION were covalently conjugated to a near-infrared fluorophore, sulfocyanine 5 (sCy5), for optical imaging and to polyethylene glycol (PEG) for improved immune stealthiness (prolonged lifetime in blood). These Stealth Fluorescent Particles (SFP) were conjugated with anti-HER2 scFv of trastuzumab in order to target HER2-overexpressing cells, such as SK-BR3 and BT-474 human breast cancer cells (Alric et al., 2018). Finally, these targeted SFP (T-SFP) were loaded with siRNA polyplexes (complexes with polycations such as chitosan and poly-L-arginine) using a protocol previously developed by our lab (Bruniaux et al., 2017). In addition to enabling siRNA complexation, the polycations favore endosomal escape of siRNA in order to reach its cytoplasmic targets (Bruniaux et al., 2017). The therapeutic target aimed in this study was survivin, a chemotherapy-induced anti-apoptotic gene. Survivin is highly and selectively expressed in a majority of human cancers, including breast cancer, representing a potential biomarker (Jha et al., 2012; Lv et al., 2010; Nassar et al., 2008). In addition, high survivin expression is correlated with chemo and radio-resistance in multiple tumor types whereas low expression enhances cell death (Guan et al., 2006; Kunze et al., 2012). In this way, survivin down-regulation through siRNA specific delivery could be considered as a therapeutic approach.

The final Targeted Stealth Magnetic siRNA Nanovectors (hereafter called TS-MSN) and the control non-targeted Stealth Magnetic siRNA Nanovectors (S-MSN) were both characterized and evaluated *in vitro*, in terms of their ability to down regulate survivin in HER2+ (SK-BR3 and BT-474 cell lines) and HER2- (MDA-MB-231 cell line) breast cancer models. In particular, we investigated the HER2 protein binding, their cellular uptake in HER2+/HER2- cells the siRNA transfection potential.

123 The latter was determined using anti-GFP siRNA delivery to the GFP-producing cells
124 or anti-survivin siRNA delivery to the non-fluorescent cancer cells.

125

126 ## *2. Materials and methods*

127 ### *2.1. Materials*

128 NHS-PEG-Maleimide (NHS-PEG-Mal, Mw 5000 Da) and sulfocyanine 5 NHS ester
129 were obtained from Rapp Polymer GmbH (Tübingen, Germany) and Lumiprobe
130 (Hannover, Germany) respectively.
131 Poly-L-arginine (MW 15.000-70.000) and high purity chitosan (MW 110.000-
132 150.000), used for S-MSN and TS-MSN formulation, were provided by Sigma–
133 Aldrich Chemie GmbH (Schnelldorf, Germany).
134 For physico-chemical characterization, model siRNA (targeted against PCSK9, sense
135 sequence GGAAGAUCAUAAUGGACAGdTdT with lower case letters representing
136 deoxyribonucleotides) were provided by Eurogentec (Angers, France). Poly-L-
137 arginine (MW 15.000-70.000) and high purity chitosan (MW 110.000-150.000; degree
138 of acetylation: ≤ 40 mol. %), used for MSN and S-MSN formulation, were from
139 Sigma–Aldrich Chemie GmbH (Schnelldorf, Germany). For transfection assay,
140 commercial transfection reagent Oligofectamine® and siRNA control were purchased
141 from Life Technologies (Paisley, UK). siRNA against survivin was purchased from
142 Sigma Aldrich Chemie GmbH (St. Quentin Fallavier, France, sense sequence
143 GUCUGGACCUCAUGUUGUUdTdT with lower case letters representing
144 deoxyribonucleotides). For gel retardation assays, loading buffer, agarose and
145 ethidium bromide were purchased from Fisher Bioreagents® (Illkirch, France). All the

culture media and supplements for cell culture were supplied by life technologies (Paisley, UK).

2.2. Nanocarriers preparation

2.2.1. Stealth fluorescent nanoparticle (SFP) and Targeted SFP (T-SFP) synthesis

T-SFP were synthesized using previously developed protocols. Briefly, SPIONs obtained using the Massart protocol were first silanized (Hervé et al., 2008). Then, silanized SPION were labelled with the fluorochrome sulfocyanine 5 NHS and functionalized with PEG leading to SFP (Alric et al., 2018; Perillo et al., 2017). In parallel, scFv anti HER2 were produced in E.coli and purified using affinity chromatography (Alric et al., 2016). Finally, SFP were functionalized with purified scFv leading to T-SFP (Alric et al., 2018, 2016). SFP as control were treated in the same conditions (reaction and purification conditions) as T-SFP.

2.2.2. Stealth magnetic siRNA nanovector (S-MSN) and targeted S-MSN (TS-MSN) preparation

TS-MSN were prepared based on a protocol previously described by Bruniaux *et al.* (Bruniaux et al., 2017). Briefly, siRNA were pre-complexed with poly-L-arginine (PLR), then added to a suspension containing T-SFP and chitosan. The amount of T-SFP (quantified by its iron content) was defined as iron/siRNA mass ratio and fixed at 10. Chitosan and PLR content were expressed by the charge ratio (CR) of positive polymer charges to negative siRNA charges. CR of chitosan/siRNA (CR_{CS}) and CR of PLR/siRNA (CR_{PS}) were respectively set to 30 and 10. S-MSN, as control, were prepared in the same conditions using SFP instead of T-SFP.

2.3. Nanocarriers' characterization

2.3.1. Size and zeta potential measurements

The mean hydrodynamic diameter and zeta potential of S-MSN and TS-MSN in suspension were determined using a Malvern Nanosizer ZS (Malvern Instruments, Malvern, UK). Before measurement, the S-MSN and TS-MSN preparations were diluted in $NaNO_3$ 0.01M at a ratio 1:25 to obtain a constant ionic strength (pH=5.6) (n=3).

2.3.2. siRNA protection assay

To analyze the siRNA protection, S-MSN and TS-MSN (at an initial siRNA concentration of 2.5 µM) were incubated with an aqueous ribonuclease A solution (1.2µg/ml, Sigma-Aldrich, Chemie GmbH, Schelldorf, Germany) at a ratio of 2:1 for 8 to 24 hours at 37°C. Afterwards, ribonuclease A was inactivated by heating the suspensions at 70°C for 30 min. An equivalent amount of free siRNA was incubated for 30 minutes and used as a positive control to check the ribonuclease A activity.

To analyze the amount of free siRNA, samples were diluted in water (Milli-Q system, Millipore, Paris, France) or aqueous heparin sodium solution (10mg/ml, Sigma-Aldrich, Chemie GmbH, Schnelldorf, Germany) and mixed with loading buffer (Agarose gel loading dye 6X) in order to deposit 20mol of siRNA per well on 1% agarose gel containing ethidium bromide. With its strong negative charge, heparin is used as control to displace complexed siRNA from S-MSN or TS-MSN. A 100 V voltage was applied for about 15 min in a Tris/acetate/EDTA buffer (TAE 1X, 40 mM acetate, EDTA 1 mM, pH 7.6). Gels were visualized and analyzed with EvolutionCapt software on a Fusion-Solo.65.WL imager (Vilbert Lourmat, Marne-la-Vallée, France).

2.3.3. Antigen-binding analysis through ELISA assay

The functionality of SFP in S-MSN formulation, and functionalized SPION (T-SFP) in TS-MSN formulation, were checked by indirect enzyme-linked immunosorbent assays (ELISA) using the HER2 protein (Sino Biologicals, Beijing, P. R. China.) as a target. scFv fragments were detected by protein L-peroxidase in the presence of chromatic substrate, 3, 30, 5, 50-tetrame-thylbenzidine (TMB), through the high affinity of protein L to the κ light chain of scFv. Briefly, HER2 protein was coated in a 96-well plate at 1 µg/mL and incubated at 37°C during 1 h. The wells were then saturated with 3% BSA-PBS for 1 h at 37°C and washed with PBS prior to incubation with an increasing concentrations of S-MSN and TS-MSN (ranging from 0 to 50 mg/L iron, 0 to 376 nM siRNA) during 1 h at 37°C. Wells were then washed and incubated with 100 µL/wells of protein L-peroxidase (Life Technologies) for 1 h at 37°C before addition to TMB substrate (Sigma-Aldrich). Enzymatic reactions were stopped with the addition of 1M H_2SO_4 and the absorbance was measured at 450 nm using a microplate reader (Biotek). Wells coloration correlated to the presence of scFv and the absorbance at 450 nm was then proportional to scFv content.

2.3.4. Immunofluorescence imaging

SK-BR3 cells, overexpressing HER2, grown on cover glasses were fixed in 4% paraformaldehyde solution for 20 min at room temperature. The cover glasses surface was saturated with a 20% fetal calf serum solution in PBS for 1 h at 37°C. The fixed cells were then incubated with 40 µL of PBS, S-MSN or TS-MSN (at an iron concentration of 267 mg/l which is equivalent to a siRNA concentration of 2000nM) all day night at 4°C in a humidified chamber box. The cover glasses were washed three times with PBS and incubated for 1h at 37 °C with protein-L-FITC (ACROBiosystems, Newark, USA) at 5 $\mu g.mL^{-1}$ for 1h at 37 °C. Cells were finally washed with PBS and placed between slide and slip cover with 10µL of Fluoromount

219 G® mounting medium. Observations were then made with a fluorescent inverted
220 microscope (Olympus, IX51).

221

222 *2.4. In vitro evaluation*

223 *2.4.1. Cell culture*

224 BT-474 and SK-BR3 human breast carcinoma cell lines with HER2 overexpression
225 were purchased from Cell Lines Service (CLS Eppelheim, Germany). BT-4747 cells
226 grow in compact, slowly growing multilayered colonies which rarely become confluent
227 and are tumorigenic in mice. In contrast, SK-BR3 cells form monolayer colonies but
228 are not tumorigenic in mice. MDA-MB231-GFP (Euromedex, Souffelweyersheim,
229 France), MDA-MB231 (ECACC, Salisbury, UK) cell lines were used as negative
230 controls as they express a low level of HER2 receptors (Alric et al., 2018). SK-BR3
231 cells were grown at 37°C/5% CO_2 in Dulbecco's Modified Eagle Medium (DMEM)
232 supplemented with 10% fetal calf serum and 1% penicillin/streptomycin. BT-474 cells
233 were grown (37°C/5% CO_2) in DMEM:Ham's F12 (1:1 mixture) supplemented with
234 insulin 1X, 10% fetal bovine serum and 1% penicillin/streptomycin. MDA-MB231 cells
235 expressing or not GFP were routinely cultured in DMEM supplemented with 10%
236 fetal calf serum, non-essential amino acid 1X and 1% penicillin/streptomycin. Culture
237 medium was changed every 48 hours and the cells were harvested using trypsin as
238 soon as 80% confluency was reached.

239 *2.4.2. Internalization studies*

240 2.4.2.1. *Flow cytometry*

24h before transfection, 25.10^3 BT-474 cells (over-expressing HER2 receptor)/wells were seeded in a 12-well plate. Transfections of 20 nM siRNA were carried out by adding a suspension of (T)S-MSN diluted in DPBS into 12-well plate containing equal parts OptiMEM serum-free medium and culture medium conventionally used for this cell line. Cells were treated with the prepared suspensions and maintained in normal growth conditions for different time points from 2 to 48h.Cells were analyzed using a FACSCalibur flow cytometer (BD Bioscience, Franklin Lakes, NJ). At least 10^4 events were collected and analyzed using the WinMDI 2.9 software.

2.4.2.2. *Confocal spectral imaging (CSI)*

For multispectral confocal imaging, the analysis of nanocarrier distribution was performed on cell-adherent cover slips. Cover glasses treated with poly-D-lysine were placed in 24-well plates. They were seeded with BT-474 cells and placed for 48 h in culture medium. The cells were then incubated with S-MSN and TS-MSN at an iron concentration of 2.66 mg/L (= 20nM siRNA concentration) for 24 h and washed three times with PBS. The cover glasses were then placed between a microscope slide and a cover slip to be scanned for CSI using a LabRAM laser scanning confocal microspectrometer (Horiba SA, Villeneuve d'Ascq, France), equipped with a 300 ‘/mm diffraction grating and a CCD detector air-cooled by Peltier effect. The sulfocyanine fluorescence was excited using a 633 nm line of a built-in He-Ne laser, under a 50 x long focal microscope objective. The laser light power at the sample was approximately 0.1 mW and the acquisition time was 20 ms per spectrum. For the analysis of adherent cells, an optical section (x-y plane) situated at half-thickness of the cell was scanned with a step of 0.8 µm that provided maps containing typically 2500 spectra. Both acquisition and treatment of multispectral maps were performed with LabSpec software version 5.

2.4.2.2. *Co-culture experiment*

For co-culture experiment 30.10^3 cells/wells and 10^4 cells/wells were respectively seeded for BT-474 and MDA-MB231/GFP considering their growth difference. Transfections of 20 nM siRNA were carried out by adding a suspension of (T)S-MSN diluted in PBS into 12-well plate containing equal parts OptiMEM serum-free medium and culture medium conventionally used for these cell lines. GFP expression of MDA-MB231 promote their discrimination with flow cytometry (FL-1 canal) in order to differentiate (T)S-MSN interaction with each cell line. Cells were treated with the prepared suspensions and maintained in normal growth conditions for different time points from 2 to 48h. Cells were analyzed using flow cytometry as described above (n = 5).

2.4.3 Efficacy studies

2.4.3.1 siRNA transfection

24h before transfection, 25.10^3 cells/well were seeded in a 12-well plate. The day of transfection, TS-MSN (at an initial siRNA concentration of 0.25 µM) were prepared and diluted in a mix of OptiMEM serum-free medium and the culture medium conventionally used for the studied cell line (1:1 v/v) in order to obtain a final siRNA concentration of 20nM. S-MSN and Oligofectamine™ (Invitrogen, Thermo Fisher Scientific, Paisley, UK) were used as controls and prepared according to the protocol described above and the manufacture recommendation, respectively. Cells were treated with the prepared suspensions and maintained in normal growth conditions for 72 h.

To validate the down-regulation functionality of siRNA formulated in TS-MSN, transfection was performed on MDA-MB231-GFP cells with anti-GFP siRNA which

specifically down-regulate GFP protein expression. For statistical analysis, the level of GFP expression was determined by flow cytometry analysis as described above.

To determine the down-regulation efficacy of our target protein survivin, BT-474 cells (overexpressing HER2 receptor) and MDA-MB231 (control) cells were transfected with TS-MSN containing anti-survivin siRNA as described above. The level of survivin protein expression was determined by Western Blotting as described below.

2.4.3.3 Western Blot (WB) –

After transfection of siRNA down-regulating survivin with the different nanocarriers for 72 h, transfected cells were washed with cold PBS and total proteins were extracted on ice by RIPA supplemented with anti-protease (Sigma-Aldrich Chemie GmbH, Schnelldorf, Germany). After 15 min centrifugation (10 000 G, 4°C) to collect supernatant, protein concentrations were determined using a bicinchoninic acid (BCA) protein assay kit (Bio-rad, Hercules, CA). The cell lysate (30 µL protein for each sample) was boiled for 5 min in SDS sample buffer and subjected to SDS-polyacrylamide gel electrophoresis (PAGE). The proteins are transferred to nitrocellulose membrane by a transfer using iBlot system. After blocking with 5 % nonfat milk at room temperature for 1 h, the membrane was incubated with the primary antibody against survivin (anti-rabbit, 1:1000, Life technologies), or glyceraldehyde-3-phosphate dehydrogenase GAPDH (anti-rabbit, 1:1000, Life technologies) at 4°C overnight. After incubating with the peroxidase conjugated secondary antibody (HRP goat to rabbit, 1:1000, Life technologies), the protein was visualized using an enhanced chemiluminescence (ECL) kit (Thermo Pierce) on a Fusion-Solo.65.WL imager (Vilbert Lourmat, Marne-la-Vallée, France) using EvolutionCapt software.

2.5. Statistical analysis

Data are expressed as mean ± SD of the variables and are compared among groups by using one-way ANOVA followed by Fisher's protected Least Significance Difference test calculated with GraphPad Prism7 software.

3. Results and Discussion

3.1. Formulation and physico-chemical characterization of targeted stealth magnetic siRNA nanovectors

Targeted Stealth Magnetic siRNA Nanovectors (called TS-MSN) were formulated combining two previously developed protocols: the synthesis protocol of Targeted Fluorescent Particles (T-SFP,(Alric et al., 2018)) and the formulation protocol of Stealth Magnetic siRNA Nanovectors (S-MSN,(Bruniaux et al., 2017)). Briefly, T-SFP, siRNA and the cationic polymers (chitosan and poly-L-arginine) were mixed together in well-defined ratio to self-assembly via electrostatic interactions and form TS-MSN. HER2-targeting scFv incorporation into S-MSN formulation using T-SFP led to an increase in physico-chemical characteristics: the hydrodynamic diameter of formulated TS-MSN doubled almost compared to S-MSN to attain about 160nm for TS-MSN and the zeta potential value of the formulation in aqueous buffer tripled almost to attain about +17mV for TS-MSN (Table 1). Both have an acceptable polydispersity index for self-assembled nanocarriers, i.e. below or around 0.3. Even if the formulation process is easy, the formulation parameters have to be carefully chosen and optimized to obtain reproducible physico-chemical parameters. Results showed that the modification of SFP with HER2 antibody fragment did not affect the

formulation parameters and led to reproducible sizes and zeta potential. Despite the increase in size and zeta potential for TS-MSN compared to S-MSN, they are still acceptable considering a future intravenous administration as the size is below 200nm and the zeta potential below 20mV in aqueous buffer (pH5.6).

To verify the protection of siRNA by our nanocarriers against enzymatic degradation, a gel electrophoresis experiment using RNAse A was performed. An aqueous siRNA solution (control) and samples of S-MSN or TS-MSN were incubated in presence and absence of RNAse A and/or heparin for 30min, 8h or 24h (Fig. 1). Heparin was added as control to liberate siRNA of the nanocarriers and to visualize complexed siRNA. Unprotected siRNA is completely degraded within 30 minutes by RNAse A as no fluorescence band is visible. In absence of RNAse A and heparin, the fluorescence intensity of free siRNA is similar in the lanes containing the control solution and in the lanes containing S-MSN (Fig. 1A) and TS-MSN (Fig. 1B). In contrast, in absence of RNAse A and heparin, no fluorescence intensity is visible for S-MSN and TS-MSN indicating complete retention of siRNA in the nanocarriers. After 8 and 24h incubation, in presence and absence of RNAse A, samples with heparin show the same fluorescence intensity of free siRNA for S-MSN and TS-MSN indicating no siRNA degradation up to 24h. These results are consistent with previous published work (Abdelrahman et al., 2017; Bruniaux et al., 2017) indicating that the modification of the SPION core with HER2-targeting scFv antibodies did not alter the siRNA protection.

To validate the specific HER2 receptor recognition by TS-MSN, an ELISA assay was performed on an immobilized recombinant protein. Results are presented in Fig. 2A. With S-MSN, there is no absorbance measured for iron concentrations up to 8 mg/L. For iron concentrations greater than 8 mg/L the absorbance increase slightly

(absorbance of 0.38 for 50 mg/L iron). This increase is related to the absorbance of the SPION and not to the association with HER2. In contrast, with TS-MSN, the absorbance start to increase for iron concentrations about 0.8 mg/L. At iron concentration of 2mg/L the absorbance is about 1 indicating a high receptor recognition. The absorbance increase in correlation with iron concentration up to a maximum absorbance for iron concentration of 50 mg/L (absorbance about 1.7), displaying the specific recognition of HER2 receptor with formulations containing HER2 antibody fragments. These results show that TS-MSN containing HER2-targeting scFv were efficiently bound to immobilized HER2 receptor while S-MSN demonstrate no association with HER2 receptor

In parallel, immunofluorescence images were realized after the incubation of S-MSN and TS-MSN with SK-BR3 cells overexpressing HER2 receptors located at the plasmic membrane (Alric et al., 2018). HER2-targeting scFv were recognized by the specific interaction between κ light chain of scFv and FITC-labeled protein L (PpL-FITC) and are represented by a green fluorescence in the images (Fig. 2B). Samples treated with TS-MSN showed an intense green fluorescence distribution on the plasma membrane demonstrating the presence of antibody fragments interacting with the HER2 proteins. In contrast, samples treated with S-MSN showed only low green fluorescence on the plasma membrane. These results are in accordance with previous results obtained with T-SFP (Alric et al., 2018). Thus, the immunofluorescence images proved that the anti-HER2 targeting with TS-MSN is still efficient even if the presence of siRNA and cationic polymers added to T-SFP

These results confirmed that TS-MSN have appropriated physico-chemical characteristics for systemic administration and that the combination of the two

protocols did not affect the characteristics of the initial properties: siRNA protection and HER2 receptor recognition.

3.2. The improved internalization through active targeting

The specific recognition of HER2 receptor with TS-MSN should improve the specific distribution inside cancer cells overexpressing this receptor. The results of internalization experiments on BT-474 cell line over-expressing HER2 receptor using flow cytometry are represented in Fig. 3A. Results showed that TS-MSN did not induce more interaction with cells for incubation time below 4 hours compared to S-MSN. Nevertheless, whereas S-MSN fluorescence with cells remained constant above 24 hours incubation, TS-MSN fluorescence continued to increase displaying a better interaction with this cell line until 48h. After 24 and 48 hours incubation, the amount of TS-MSN found inside the BT-474 cells is respectively 1.4 and 2.2 times higher compared to the amount of S-MSN in the same cell line. This result was confirmed and completed with multispectral confocal imaging. After 24 hours incubation, TS-MSN had a massive internalization into cytoplasmic compartment with a homogenous distribution (Fig. 3B). T-SFP (red) and siRNA-alexa488 (green) were represented with high intensity signal suggesting that the nanovectors allow the delivery of siRNA inside the cells with high efficacy. In the same conditions with S-MSN, despite an accumulation into cytoplasmic compartment, the intensity signal remained weaker confirming the contribution of active targeting with TS-MSN.

To ensure the privileged TS-MSN distribution into cell lines overexpressing HER2 receptor, internalization studies on cellular co-culture were performed (Fig. 4). S-MSN and TS-MSN were incubated for increasing incubation times into a mixed culture of MDA-MB231/GFP (HER2-) and BT-474 (HER2+) cells. The different cell

411 lines were discriminated through the green fluorescent protein (GFP) expression of
412 MDA-MB231/GFP in order to compare nanocarrier interactions with cells depending
413 on their HER2 receptor expression (Fig. 4A).

414 For TS-MSN, the fluorescence signal increased significantly over time in MDA-
415 MB231/GFP cells up to 4h ($p < 0.001$) with a threshold between 4 and 24h and a
416 slight increase between 24 and 48h ($p< 0.01$). In BT-474 cells, the fluorescence
417 signal increased continuously between 2 and 48h but without any threshold ($p <$
418 0.001 up to 24h and $p < 0.01$ between 24 and 48h) (Fig. 4B). These results displayed
419 more interaction between cells overexpressing HER2 receptors and nanocarriers
420 with active targeting (TS-MSN). In contrast, with S-MSN the fluorescence signal
421 increased significantly in both cell lines between 2 and 24h with a threshold after 24h
422 ($p < 0.001$ for all points except at 24h for MDA-MB231/ GFP cells where $p < 0.01$),
423 indicating that the entry of S-MSN inside both cell lines is similar.

424 However, at all time points the fluorescence signal intensity measured on cells
425 incubated with TS-MSN is significantly higher than that measured on cells incubated
426 with S-MSN indicating more interaction between TS-MSN with cells. The difference
427 between TS-MSN and S-MSN was the same in both cell lines after 2h incubation (3.4
428 times). This phenomenon can be explained by the highly positive zeta potential value
429 of TS-MSN compared to S-MSN allowing stronger interaction with the plasmic
430 membrane (Table 1). However, this difference appeared to be higher after longer
431 incubation: a fluorescence intensity 4 times higher for 4h incubation, and respectively
432 3.2 and 3.7 times higher for 24h et 48h indicating a more pronounced internalization
433 of TS-MSN in BT-474 thanks to the overexpression of the HER2 receptor.

In summary, TS-MSN containing HER2-targeting scFv showed (i) the specific HER2 receptor recognition in BT-474 cells while S-MSN demonstrated no visible distinction between both cell lines, (ii) an enhanced internalization in BT-474 (HER2+) cells compared to MDA-MB231/GFP cells for long term incubation (> 24 hours).

These results are in accordance with our previous study performed on T-SFP (Alric *et al*, 2018) and with other studies that have previously reported the improved delivery of nanocarriers to the tumor sites by conjugation of HER2 antibody to the delivery carriers. Kievit *et al.* developed multifunctional superparamagnetic iron oxide nanoparticles containing trastuzumab antibody for active targeting and displayed the efficient targeting effect on HER2 expressing mouse mammary carcinoma (MMC) cells *in vitro* and *in vivo* in a transgenic mouse model (Kievit et al., 2012). In this study on HER2 expressing MMC, nanocarriers (50 µg/mL nanoparticles) containing trastuzumab antibodies led to an internalization two times higher after 2 hours of treatments compared to non-functionalized nanoparticles (Kievit et al., 2012). In the same way, *Choi et al.* described that the extent of cellular uptake of anti-HER2 antibody-conjugated iron oxide nanoparticles (150 µg/mL iron) was approximately 5 times higher in HER2-positive cells than in HER2-negative cells at all time points (Choi et al., 2015). Despite a considerably lower iron concentration (ca. 2.67 µg/mL), our study reports an impact of active targeting on HER2-overexpressed BT-474 cells after comparison with MDA-MB231/GFP cells.

3.3. The impact of active targeting on down-regulation efficiency after siRNA transfection

To verify the down-regulation efficiency of TS-MSN, flow cytometry experiments were performed on a MDA-MB231/GFP model using nanocarriers formulated with siRNA against GFP (Fig. 5A). Results demonstrated GFP down-regulation efficiency about 60% after siRNA transfection with TS-MSN, at the same level than S-MSN or commercial lipoplex formulation, Oligofectamine®. These results are in accordance with previous obtained results for S-MSN (Bruniaux et al., 2017).

To check the down-regulation efficiency of survivin by TS-MSN, Western Blot experiments were performed on MDA-MB231 cells using nanocarriers formulated with siRNA against survivin (Fig. 5B). Results demonstrated survivin down-regulation efficiency about 70% after siRNA transfection with TS-MSN, at a similar level as S-MSN. Surprisingly, commercial lipoplex formulation, Oligofectamine® inhibited the survivin expression only about 15%.

These results indicate that modification of SFP by antibodies fragments grafting to obtain T-SFP, in order to upgrade S-MSN to TS-MSN, did not alter the down-regulation efficiency on this HER2 negative model.

To verify the impact of the observed active targeting of TS-MSN on the specific down-regulation, transfection on BT-474 (HER2+) cells was performed in order to down-regulate survivin expression. After 72 hours transfection of siSurvivin with Oligofectamine®, S-MSN and TS-MSN, survivin protein level was analyzed through western-blot and compared to transfection with siControl (Fig. 5C). As expected, transfection with siControl did not provide any survivin protein down-regulation. As in the previous experiment on MDA-MB231 cells, siSurvivin transfection with Oligofectamine® enabled only about 15% survivin down-regulation whereas S-MSN induced about 70% down-regulation in the same conditions. With active targeting

allowed by TS-MSN, survivin down-regulation was improved to about 90% demonstrating a direct contribution of HER2-targeting scFv integration in the formulation. Thus TS-MSN provide efficient down-regulation efficiency of survivin on BT-474 cells *in vitro*.

The study was performed with siRNA targeting GFP and survivin showing significant protein down-regulation and indicating the adaptability of the delivery system to many target genes. Additionally, results show that the functionalization of T-SFP with scFv did not disturb the optimized formulation protocol of S-MSN indicating the adaptability of the delivery system to other cell types.

The correlation between selective targeting and down-regulation efficiency was also demonstrated by Jiang *et al.*: siRNA transfection (from 10 to 40 nM) with e23sFv-9R protein, allowing specific HER2 recognition, induced significant CXCR4 expression decrease in BT-474 cells (HER2+) whereas no obvious change in MDA-MB231 cells (HER2-) was observed (Jiang et al., 2015). Despite the difference in both delivery system and siRNA target, the same behavior were observed with the specific antibody fragment grafting. Such a correlation was also observed with other targeting ligands on other cell types using nanovectors more similar to ours. For example, Veiseh *et al.* used SPION coated with PEG-grafted chitosan and PEI which were functionalized with siRNA and the tumor-targeting ligand, chlorotoxin (CTX). They showed that CTX-targeted nanovectors were internalized by C6 tumor cells 2-fold more than untargeted nanovectors and that the gene knock-down was correlated (35% reduction in GFP expression with non-targeted nanovectors vs 62% with CTX-targetd nanovectors) (Veiseh et al., 2010). However, to achieve this down-regulation efficiency, they have to use 7.5 times more siRNA, compared to the present study. Another example is the publication of Yang *et al.* who functionalized their SPION via

electrostatic absorption of PEI and Gal-PEG-NH_2 (using galactose as targeting ligand) and loaded the obtained Gal-PEI-SPION with siRNA via electrostatic interactions. They emphasized the importance of nanoparticles protecting cargo siRNA from nuclease degradation during *in vivo* siRNA delivery. Their serum stability study showed no siRNA degradation up to 48h. Furthermore, cy5-siRNA loaded Gal-PEI-SPIO nanoparticles were still observed with strong fluorescence intensity 24h after intravenous injection into C57BL/6 tumor-bearing mice showing the successful complexation of the siRNA into Gal-PEI-SPIO nanoparticles with high protection efficiency. They showed that the tumor volume, the liver/body weight ratio and the mRNA levels were significantly reduced using siRNA against c-Met compared to a negative control siRNA after repeated intravenous administration in an orthotopic hepatocellular carcinoma mouse model (Yang et al., 2018). However, they did not compare their formulation with a non-targeted formulation.

The main advantage of using SPION as delivery system is related to their theranostic properties, i.e. their possible monitoring using imaging techniques such as MRI thus allowing to combine their diagnostic and their therapeutic functions. The above cited examples and the promising results presented here (physico-chemical characteristics of the nanocarriers compatible with an intravenous administration, siRNA protection against nuclease degradation up to 24h, active targeting and efficient down-regulation *in vitro*) encourage us to continue towards *in vivo* preclinical assays. Moreover, *in vivo*, active cancer targeting through HER2 recognition, combined to an enhanced permeability and retention (EPR) effect in tumor environment, should promote specific biodistribution and improved down-regulation efficiency compared to control non-targeted nanovectors.

4. Conclusion

In this study, Targeted Stealth Magnetic siRNA Nanovectors (TS-MSN), were developed as alternative to existing HER2 cancer therapies in the objective to achieve a maximal therapeutic benefit. Therefore T-SFP functionalized with trastuzumab scFv (targeting HER2) were combined with S-MSN (for efficient siRNA delivery) and loaded with siRNA targeting survivin (highly expressed in cancers such as HER2 breast cancer). The main conclusions of our developed delivery system are that: 1) the formulation is rapid and simple 2) this delivery system can be adapted to many target genes, 3) the transfection efficacy is very high even if the nanovector is not targeted (S-MSN), 4) the active targeting with anti-HER2 antibody fragment increased the uptake of TS-MSN into the cells and especially in HER2 overexpressing cells, 5) the gene silencing effect of anti-survivin siRNA is even stronger for TS-MSN on cells that overexpressed the HER2 receptor.

Acknowledgments

This work was supported by the “Institut National du Cancer (INCa)”, the “Fondation ARC” and the “Ligue Nationale Contre le Cancer (LNCC)” (ARC_INCa_LNCC_7636), the "Région Centre-Val de Loire" (NCIS Project) and the “Cancéropole Grand Ouest”. "This work has been funded with support from the French Higher Education and Research ministry under the program “Investissements d’avenir” Grant Agreement: LabEx MAbImprove ANR-10-LABX-53–01."The authors would like to thank Isabelle Dimier-Poisson and Nathalie Moire (UMR INRA 1282, team of “Infectiologie et Santé Publique”, University François Rabelais of Tours) for their help with flow cytometry experiments and Lizzy Angevin for skillful technical support with cells.

References

Abdelrahman, M., Douziech Eyrolles, L., Alkarib, S.Y., Hervé-Aubert, K., Ben Djemaa, S., Marchais, H., Chourpa, I., David, S., 2017. siRNA delivery system based on magnetic nanovectors: Characterization and stability evaluation. Eur. J. Pharm. Sci. Off. J. Eur. Fed. Pharm. Sci. 106, 287–293. https://doi.org/10.1016/j.ejps.2017.05.062

Allen, T.M., 2002. Ligand-targeted therapeutics in anticancer therapy. Nat. Rev. Cancer 2, 750–763. https://doi.org/10.1038/nrc903

Alric, C., Aubrey, N., Allard-Vannier, É., di Tommaso, A., Blondy, T., Dimier-Poisson, I., Chourpa, I., Hervé-Aubert, K., 2016. Covalent conjugation of cysteine-engineered scFv to PEGylated magnetic nanoprobes for immunotargeting of breast cancer cells. RSC Adv. 6, 37099–37109. https://doi.org/10.1039/C6RA06076E

Alric, C., Hervé-Aubert, K., Aubrey, N., Melouk, S., Lajoie, L., Même, W., Même, S., Courbebaisse, Y., Ignatova, A.A., Feofanov, A.V., Chourpa, I., Allard-Vannier, E., 2018. Targeting HER2-breast tumors with scFv-decorated bimodal nanoprobes. J. Nanobiotechnology 16, 18. https://doi.org/10.1186/s12951-018-0341-6

Anhorn, M.G., Wagner, S., Kreuter, J., Langer, K., von Briesen, H., 2008. Specific targeting of HER2 overexpressing breast cancer cells with doxorubicin-loaded trastuzumab-modified human serum albumin nanoparticles. Bioconjug. Chem. 19, 2321–2331. https://doi.org/10.1021/bc8002452

Bruniaux, J., Djemaa, S.B., Hervé-Aubert, K., Marchais, H., Chourpa, I., David, S., 2017. Stealth magnetic nanocarriers of siRNA as platform for breast cancer theranostics. Int. J. Pharm. https://doi.org/10.1016/j.ijpharm.2017.05.022

Chattopadhyay, N., Fonge, H., Cai, Z., Scollard, D., Lechtman, E., Done, S.J., Pignol, J.-P., Reilly, R.M., 2012. Role of antibody-mediated tumor targeting and route of administration in nanoparticle tumor accumulation in vivo. Mol. Pharm. 9, 2168–2179. https://doi.org/10.1021/mp300016p

Choi, W.I., Lee, J.H., Kim, J.-Y., Heo, S.U., Jeong, Y.Y., Kim, Y.H., Tae, G., 2015. Targeted antitumor efficacy and imaging via multifunctional nano-carrier conjugated with anti-HER2 trastuzumab. Nanomedicine Nanotechnol. Biol. Med. 11, 359–368. https://doi.org/10.1016/j.nano.2014.09.009

Ferlay, J., Soerjomataram, I., Dikshit, R., Eser, S., Mathers, C., Rebelo, M., Parkin, D.M., Forman, D., Bray, F., 2015. Cancer incidence and mortality worldwide: Sources, methods and major patterns in GLOBOCAN 2012. Int. J. Cancer 136, E359–E386. https://doi.org/10.1002/ijc.29210

Guan, H.-T., Xue, X.-H., Dai, Z.-J., Wang, X.-J., Li, A., Qin, Z.-Y., 2006. Down-regulation of survivin expression by small interfering RNA induces pancreatic cancer cell apoptosis and enhances its radiosensitivity. World J. Gastroenterol. 12, 2901–2907.

Hervé, K., Douziech-Eyrolles, L., Munnier, E., Cohen-Jonathan, S., Soucé, M., Marchais, H., Limelette, P., Warmont, F., Saboungi, M.L., Dubois, P., Chourpa, I., 2008. The development of stable aqueous suspensions of PEGylated SPIONs for biomedical applications. Nanotechnology 19, 465608. https://doi.org/10.1088/0957-4484/19/46/465608

Jee, J.-P., Na, J.H., Lee, S., Kim, S.H., Choi, K., Yeo, Y., Kwon, I.C., 2012. Cancer targeting strategies in nanomedicine: Design and application of chitosan nanoparticles. Curr. Opin. Solid State Mater. Sci., Polymeric Nanomedicine 16, 333–342. https://doi.org/10.1016/j.cossms.2013.01.002

Jha, K., Shukla, M., Pandey, M., 2012. Survivin expression and targeting in breast cancer. Surg. Oncol. 21, 125–131. https://doi.org/10.1016/j.suronc.2011.01.001

602 Jiang, K., Li, J., Yin, J., Ma, Q., Yan, B., Zhang, X., Wang, Lei, Wang, Lifeng, Liu, T., Zhang, Y., Fan, Q.,
603 Yang, A., Qiu, X., Ma, B., 2015. Targeted delivery of CXCR4-siRNA by scFv for HER2(+) breast
604 cancer therapy. Biomaterials 59, 77–87. https://doi.org/10.1016/j.biomaterials.2015.04.030
605 Kaczmarek, J.C., Kowalski, P.S., Anderson, D.G., 2017. Advances in the delivery of RNA therapeutics:
606 from concept to clinical reality. Genome Med. 9, 60. https://doi.org/10.1186/s13073-017-
607 0450-0
608 Kievit, F.M., Stephen, Z.R., Veiseh, O., Arami, H., Wang, T., Lai, V.P., Park, J.O., Ellenbogen, R.G., Disis,
609 M.L., Zhang, M., 2012. Targeting of primary breast cancers and metastases in a transgenic
610 mouse model using rationally designed multifunctional SPIONs. ACS Nano 6, 2591–2601.
611 https://doi.org/10.1021/nn205070h
612 Kunze, D., Erdmann, K., Froehner, M., Wirth, M.P., Fuessel, S., 2012. siRNA-mediated inhibition of
613 antiapoptotic genes enhances chemotherapy efficacy in bladder cancer cells. Anticancer Res.
614 32, 4313–4318.
615 Ledford, H., 2018. Gene-silencing technology gets first drug approval after 20-year wait. Nature 560,
616 291–292. https://doi.org/10.1038/d41586-018-05867-7
617 Lv, Y.-G., Yu, F., Yao, Q., Chen, J.-H., Wang, L., 2010. The role of survivin in diagnosis, prognosis and
618 treatment of breast cancer. J. Thorac. Dis. 2, 100–110.
619 Marty, M., Cognetti, F., Maraninchi, D., Snyder, R., Mauriac, L., Tubiana-Hulin, M., Chan, S., Grimes,
620 D., Antón, A., Lluch, A., Kennedy, J., O'Byrne, K., Conte, P., Green, M., Ward, C., Mayne, K.,
621 Extra, J.-M., 2005. Randomized phase II trial of the efficacy and safety of trastuzumab
622 combined with docetaxel in patients with human epidermal growth factor receptor 2-
623 positive metastatic breast cancer administered as first-line treatment: the M77001 study
624 group. J. Clin. Oncol. Off. J. Am. Soc. Clin. Oncol. 23, 4265–4274.
625 https://doi.org/10.1200/JCO.2005.04.173
626 Nassar, A., Sexton, D., Cotsonis, G., Cohen, C., 2008. Survivin expression in breast carcinoma:
627 correlation with apoptosis and prognosis. Appl. Immunohistochem. Mol. Morphol. AIMM 16,
628 221–226. https://doi.org/10.1097/PAI.0b013e3180c317bc
629 Perillo, E., Hervé-Aubert, K., Allard-Vannier, E., Falanga, A., Galdiero, S., Chourpa, I., 2017. Synthesis
630 and in vitro evaluation of fluorescent and magnetic nanoparticles functionalized with a cell
631 penetrating peptide for cancer theranosis. J. Colloid Interface Sci. 499, 209–217.
632 https://doi.org/10.1016/j.jcis.2017.03.106
633 Santos, S.B., Sousa Lobo, J.M., Silva, A.C., 2019. Biosimilar medicines used for cancer therapy in
634 Europe: a review. Drug Discov. Today 24, 293–299.
635 https://doi.org/10.1016/j.drudis.2018.09.011
636 Slamon, D.J., Godolphin, W., Jones, L.A., Holt, J.A., Wong, S.G., Keith, D.E., Levin, W.J., Stuart, S.G.,
637 Udove, J., Ullrich, A., 1989. Studies of the HER-2/neu proto-oncogene in human breast and
638 ovarian cancer. Science 244, 707–712.
639 Slavoff, S.A., Saghatelian, A., 2012. Discovering ligand-receptor interactions. Nat. Biotechnol. 30,
640 959–961. https://doi.org/10.1038/nbt.2373
641 Steinhauser, I., Spänkuch, B., Strebhardt, K., Langer, K., 2006. Trastuzumab-modified nanoparticles:
642 optimisation of preparation and uptake in cancer cells. Biomaterials 27, 4975–4983.
643 https://doi.org/10.1016/j.biomaterials.2006.05.016
644 Swain, S.M., Baselga, J., Kim, S.-B., Ro, J., Semiglazov, V., Campone, M., Ciruelos, E., Ferrero, J.-M.,
645 Schneeweiss, A., Heeson, S., Clark, E., Ross, G., Benyunes, M.C., Cortés, J., CLEOPATRA Study
646 Group, 2015. Pertuzumab, trastuzumab, and docetaxel in HER2-positive metastatic breast
647 cancer. N. Engl. J. Med. 372, 724–734. https://doi.org/10.1056/NEJMoa1413513
648 Tatiparti, K., Sau, S., Kashaw, S.K., Iyer, A.K., 2017. siRNA Delivery Strategies: A Comprehensive
649 Review of Recent Developments. Nanomater. Basel Switz. 7.
650 https://doi.org/10.3390/nano7040077
651 Veiseh, O., Kievit, F.M., Fang, C., Mu, N., Jana, S., Leung, M.C., Mok, H., Ellenbogen, R.G., Park, J.O.,
652 Zhang, M., 2010. Chlorotoxin bound magnetic nanovector tailored for cancer cell targeting,

imaging, and siRNA delivery. Biomaterials 31, 8032–8042. https://doi.org/10.1016/j.biomaterials.2010.07.016

Verma, S., Miles, D., Gianni, L., Krop, I.E., Welslau, M., Baselga, J., Pegram, M., Oh, D.-Y., Diéras, V., Guardino, E., Fang, L., Lu, M.W., Olsen, S., Blackwell, K., EMILIA Study Group, 2012. Trastuzumab emtansine for HER2-positive advanced breast cancer. N. Engl. J. Med. 367, 1783–1791. https://doi.org/10.1056/NEJMoa1209124

Wang, T., Shigdar, S., Shamaileh, H.A., Gantier, M.P., Yin, W., Xiang, D., Wang, L., Zhou, S.-F., Hou, Y., Wang, P., Zhang, W., Pu, C., Duan, W., 2017. Challenges and opportunities for siRNA-based cancer treatment. Cancer Lett. 387, 77–83. https://doi.org/10.1016/j.canlet.2016.03.045

Yang, Z., Duan, J., Wang, J., Liu, Q., Shang, R., Yang, X., Lu, P., Xia, C., Wang, L., Dou, K., 2018. Superparamagnetic iron oxide nanoparticles modified with polyethylenimine and galactose for siRNA targeted delivery in hepatocellular carcinoma therapy. Int. J. Nanomedicine 13, 1851–1865. https://doi.org/10.2147/IJN.S155537

668 **Table 1.** Physico-chemical characteristics of S-MSN and TS-MSN

	Hydrodynamic diameter *nm*	Polydispersity	Zeta potential *mV*
TS-MSN	157 ± 22	0.30 ± 0.04	+17 ± 4
S-MSN	73 ± 6	0.17 ± 0.03	+5 ± 2

669

670

Figure captions:

Fig. 1. Gel retardation assay demonstrating the siRNA protection against enzymatic degradation. siRNA formulated in S-MSN (**A**) or TS-MSN (**B**) in presence or absence of RNAse A and/or heparin after 8 and 24h incubation compared to naked siRNA incubated for 30 min. Lanes without heparin show free siRNA amount and lanes with heparin show total siRNA amount in the sample.

Fig. 2. HER2 protein recognition of S-MSN and TS-MSN. **A**: Indirect ELISA test of the immunoreactivity of TS-MSN (red curve) and S-MSN (green curve). **B**: Immunofluorescence images of SK-BR3 breast cancer cells incubated with TS-MSN and S-MSN (detection with PpL-FITC) and white light images to visualize the cells.

Fig. 3. Uptake of TS-MSN and S-MSN in BT-474 (HER2+) cells . **A**: Uptake kinetics of TS-MSN (red curve) and S-MSN (green curve). **B**: Confocal spectral imaging data showing the fluorescence of the sulfocyanine labelled nanosystems (red) and the Alexa-488 labelled siRNA (green) after 24h of incubation. Representative spectra of both fluorochromes (emission maximum: 525 for Alexa-488 and 710 nm for Sulfocyanine-5) are shown below.

Fig. 4 : Uptake kinetics of TS-MSN and S-MSN in a co-culture of BT-474 and MDA-MB231-GFP cells. **A**. Schematic representation of the co-culture and cytometry separation of the two cell lines according to green fluorescence intensity. **B**. Representation of the sulfocyanine fluorescence ratio found in BT-474 versus MDA-MB231-GFP cell lines after incubation of TS-MSN (left) and S-MSN (right) according time (2 – 48h). *: $p<0.05$; **: $p<0.01$; ***: $p< 0.001$ correspond to the comparison between MDA-MB231/GFP and BT-474 for a same incubation time. ##: $p<0.01$; ###: $p<0.001$ correspond to the comparison with the previous incubation time for the same cell line.

Fig. 5. Down-regulation efficiency of S-MSN and TS-MSN. A. GFP fluorescence expression in MDA-MB-231/GFP cells either untreated (Cell MDA-MB-231/GFP) or treated with oligofectamine®, S-MSN or TS-MSN formulated with anti GFP siRNA. **B.** Western Blot membranes of survivin expression in MDA-MB-231 cells either untreated (Cell MDA-MB-231) or treated with oligofectamine®, S-MSN or TS-MSN formulated with anti-survivin siRNA. **C.** Survivin down-regulation in BT474 cells. Western Blot membranes of survivin expression in BT474 cells either untreated (Cell

703 BT474) or treated with oligofectamine®, S-MSN or TS-MSN formulated with either
704 anti-survivin siRNA or a control siRNA.

705

A

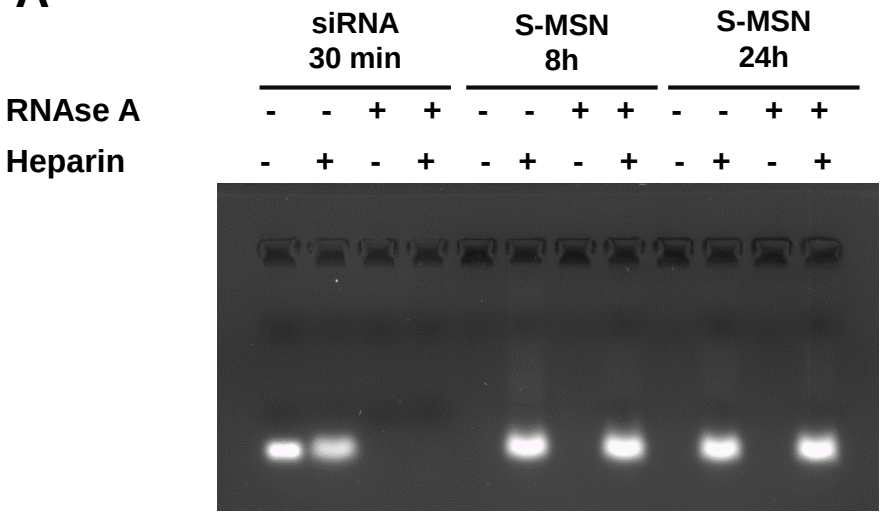
siRNA
30 min
S-MSN
8h
S-MSN
24h
RNAse A
- - + + - - + + - - + +
Heparin
- + - + - + - + - + - +

B

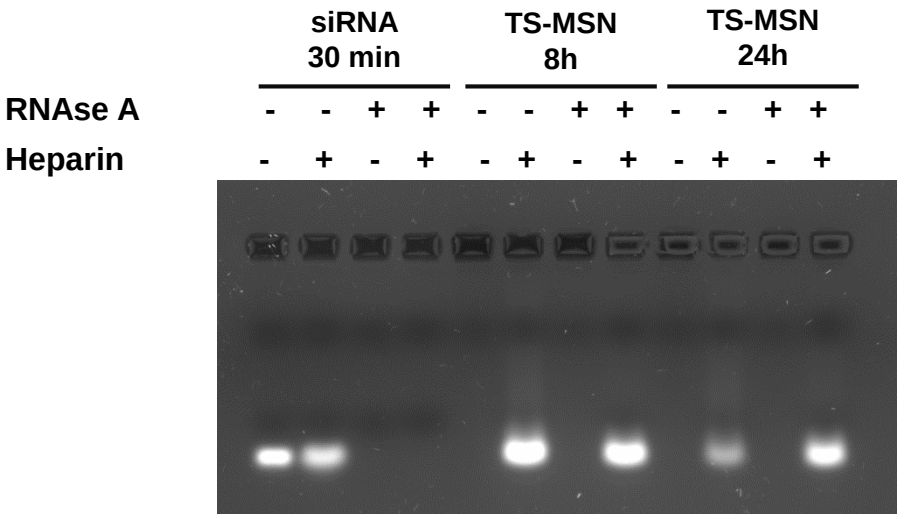
siRNA
30 min
TS-MSN
8h
TS-MSN
24h
RNAse A
- - + + - - + + - - + +
Heparin
- + - + - + - + - + - +

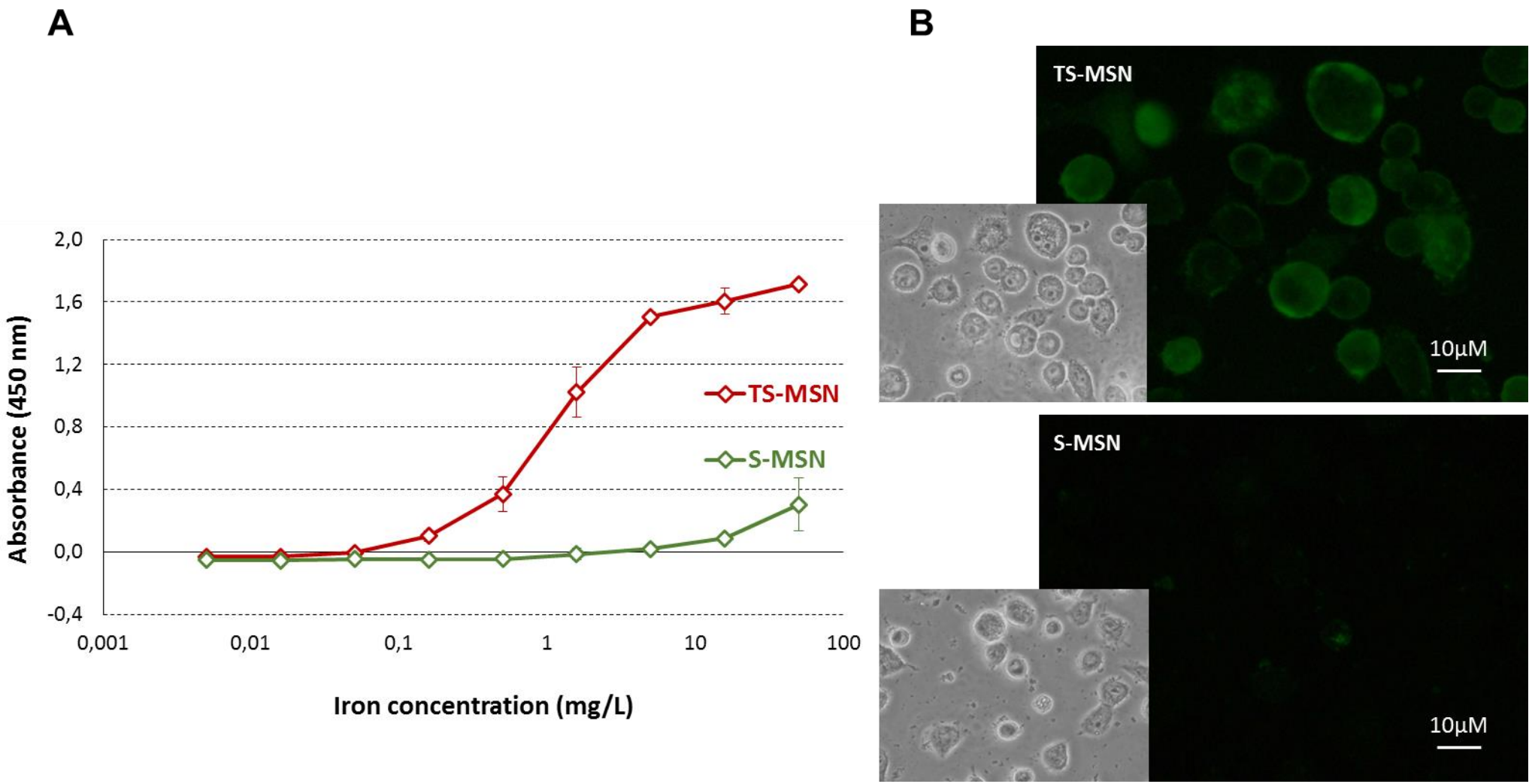
A
B
Absorbance (450 nm)
2,0
1,6
1,2
0,8
0,4
0,0
-0,4
0,001
0,01
0,1
1
10
100
Iron concentration (mg/L)
TS-MSN
S-MSN
TS-MSN
10µM
S-MSN
10µM

A

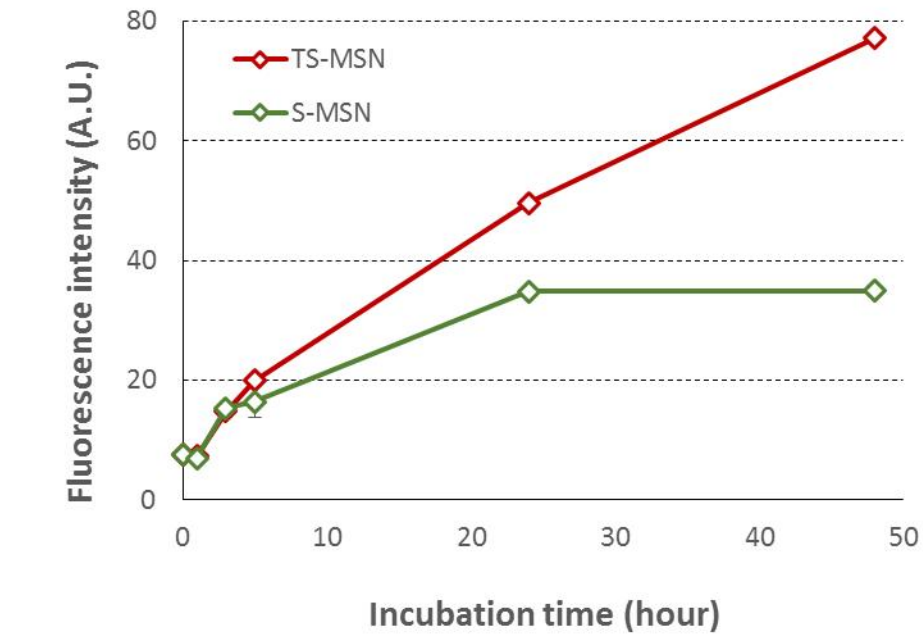
80
60
40
20
0
TS-MSN
S-MSN
Fluorescence intensity (A.U.)
0
10
20
30
40
50
Incubation time (hour)

B

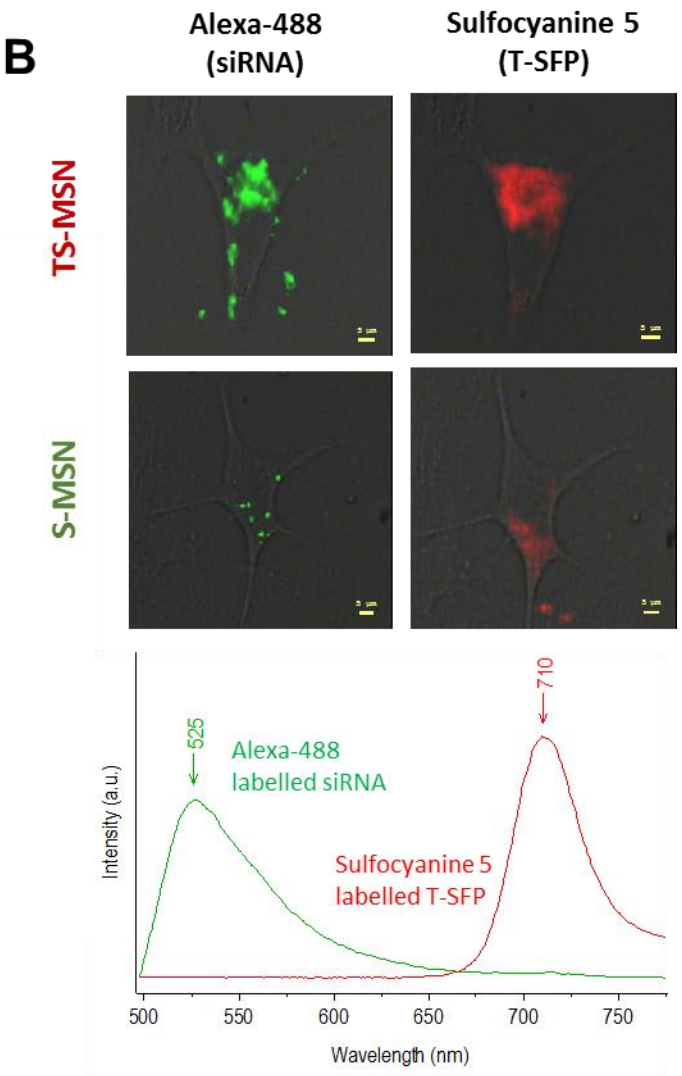
Alexa-488
(siRNA)
Sulfocyanine 5
(T-SFP)
TS-MSN
S-MSN
525
710
Alexa-488
labelled siRNA
Sulfocyanine 5
labelled T-SFP
Intensity (a.u.)
500
550
600
650
700
750
Wavelength (nm)

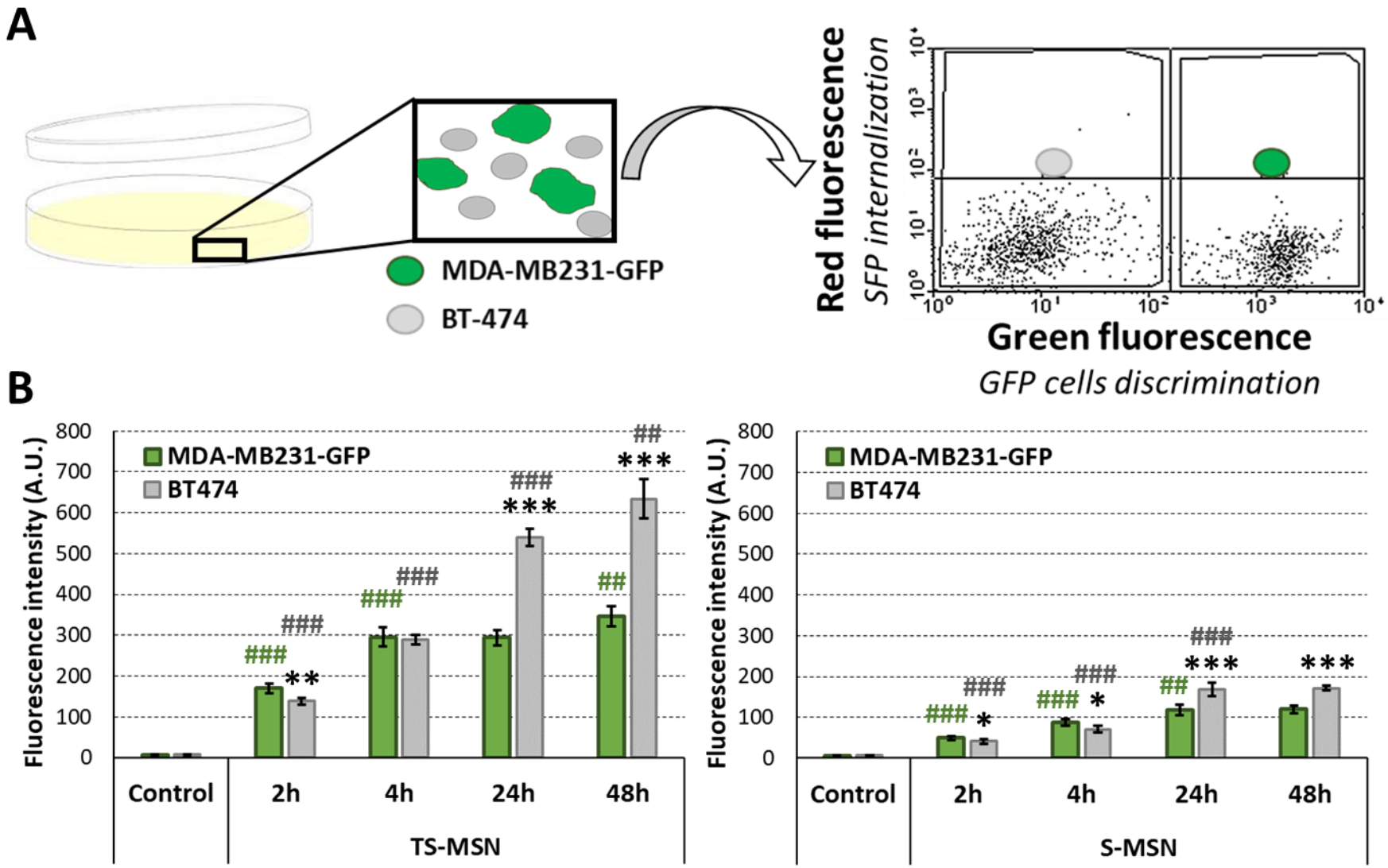
A
MDA-MB231-GFP
BT-474
Red fluorescence
SFP internalization
Green fluorescence
GFP cells discrimination
B
Fluorescence intensity (A.U.)
MDA-MB231-GFP
BT474
Control
2h
4h
24h
48h
TS-MSN
S-MSN

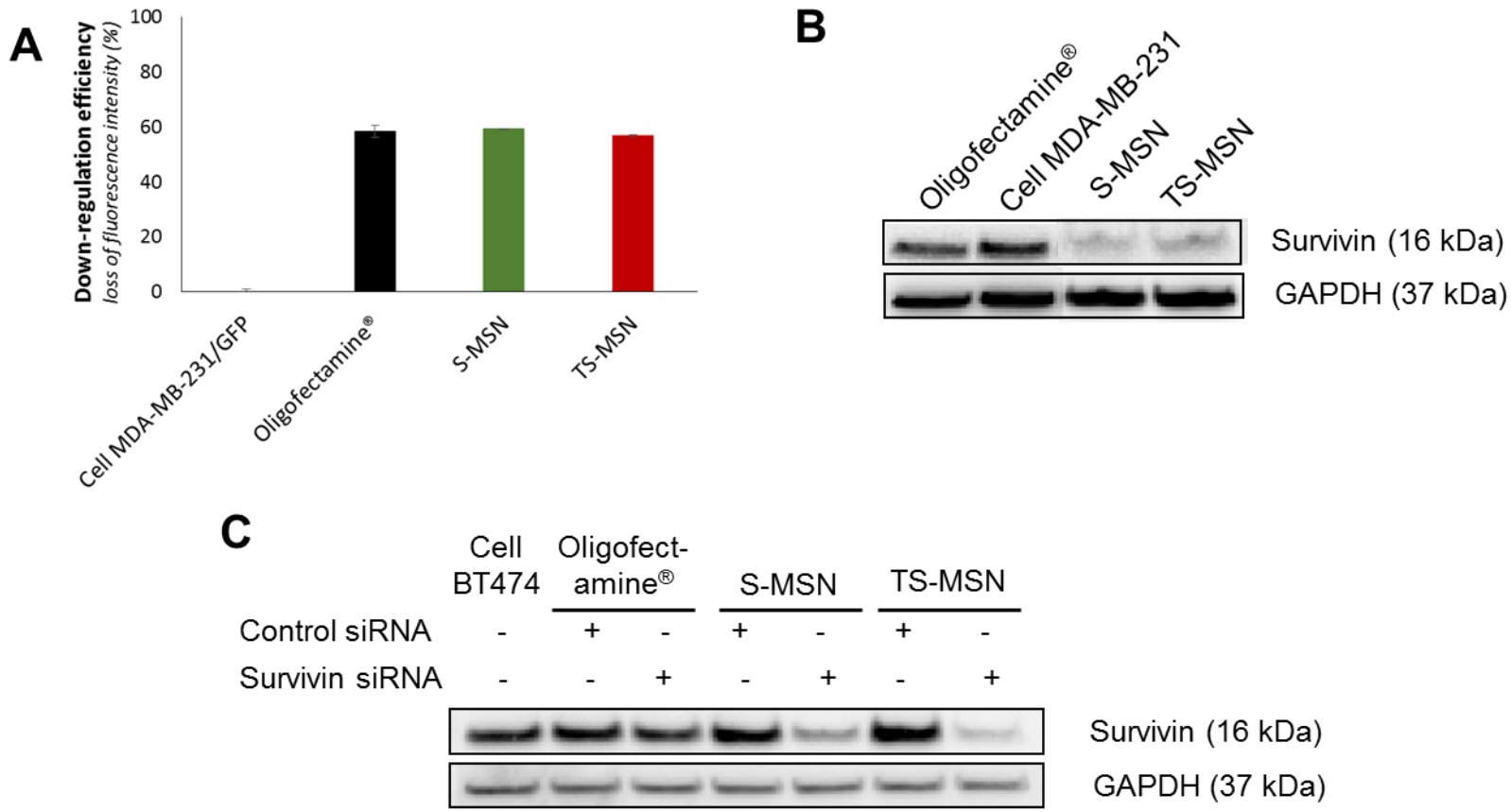
A
Down-regulation efficiency
loss of fluorescence intensity (%)
100
80
60
40
20
0
Cell MDA-MB-231/GFP
Oligofectamine®
S-MSN
TS-MSN
B
Oligofectamine®
Cell MDA-MB-231
S-MSN
TS-MSN
Survivin (16 kDa)
GAPDH (37 kDa)
C
Cell BT474
Oligofect-amine®
S-MSN
TS-MSN
Control siRNA - + - + - + -
Survivin siRNA - - + - + - +
Survivin (16 kDa)
GAPDH (37 kDa)

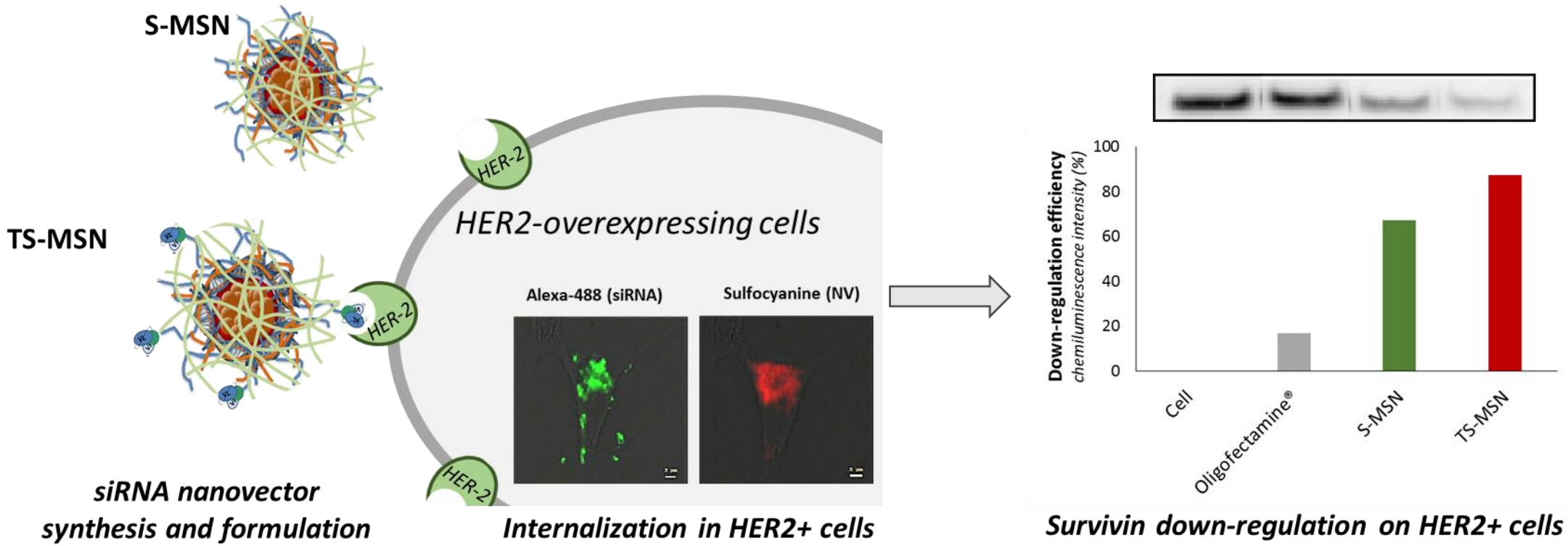

siRNA nanovector synthesis and formulation

Internalization in HER2+ cells

Survivin down-regulation on HER2+ cells